To appear in:
International Journal of Nano Dimension (Int. J. Nano Dimens.)

Online ISSN: 2228-5059 Print ISSN: 2008-8868

Dates:
Received: 04 May 2025
Revised: 23 July 2025
Accepted: 30 August 2025

DOI: https://doi.org/10.57647/ijnd-2026-1702-06

Research Paper

The effect of chitosan nanoparticles loaded with *Ganoderma lucidum* polysaccharide content on the expression of Bax and Bcl-2 genes and induction of apoptosis in the PC3 cell line

Mohaddeseh Larypoor[1,*], Mahnaz Joodi Ghareh Shiran[2], Hoora Dadgostar[3], Maryam Bikhof Torbati[4], Shahrzad Sadeghi Amjad[5]

[1] *Department of Microbiology, Faculty of Biological Sciences, NT.C., Islamic Azad University, Tehran*

[2] *Department of Microbiology, Faculty of Biological Sciences, NT.C., Islamic Azad University, Tehran, Iran*
[3] *Department of Microbiology, Faculty of Biological Sciences, NT.C., Islamic Azad University, Tehran, Iran*

[4] *Department of Biology, Faculty of Biological Sciences, YI.C., Islamic Azad University, Tehran, Iran*

[5] *Department of Microbiology, Faculty of Biological Sciences, CT.C., Islamic Azad University, Tehran, Iran*

Corresponding Author: **Mohaddeseh Larypoor**, m.larypoor@iau.ir

Abstract

Research into anti-cancer compounds from natural sources, such as *Ganoderma lucidum* and chitosan, and the development of their delivery systems, is a highly promising field. This study focused on developing nanocarriers of *Ganoderma lucidum* polysaccharides-chitosan and evaluating their effects on the expression of the Bax and Bcl-2 genes in the PC3 cell line. The extraction of polysaccharides from *Ganoderma lucidum* involved heating the material in water at 70 °C, followed by treatment with 96% ethanol and subsequent protein removal to purify the polysaccharides. These polysaccharides were successfully incorporated into chitosan nanoparticles via ion-exchange copolymerization. Scanning electron microscopy (SEM) and Fourier-transform infrared spectroscopy (FTIR) were utilized to examine the morphology and chemical properties of the synthesized nanoparticles. The effects of the chitosan-polysaccharide nanoparticles and free polysaccharides on gene expression were assessed using real-time PCR after treating PC3 cells with various concentrations. The results showed that the nanoparticles and polysaccharides increased Bax gene expression by 4.6-fold and 5.56-fold, respectively, while decreasing Bcl-2 expression by 0.64-fold and 0.81-fold, respectively. These observed changes indicate that apoptosis was induced in PC3 cells. Nanoparticles composed of polysaccharides and chitosan show promise for future prostate cancer therapies; however, additional in vitro and in vivo studies are necessary.

Keywords: *Bax*; *Bcl-2; Chitosan*; *Ganoderma lucidum*; *Nanoparticle*; *Prostate cancer*; *PC3*.

1. Introduction

Scientific research continues to focus on cancer, the second leading cause of death worldwide. Prostate cancer is the fifth leading cause of cancer-related deaths among men. Various genetic predispositions and environmental influences, including dietary habits and lifestyle choices, collectively affect the risk of developing prostate cancer [1]. Factors such as awareness, early diagnosis, and the use of novel drug delivery methods to improve therapeutic efficacy and reduce side effects are important in controlling prostate cancer [2]. The study of apoptotic mechanisms and their associated factors is a central focus of anticancer research. Apoptosis is a complex process regulated by gene products, particularly Bcl-2, Bax, and caspases [3, 4]. The initiation of apoptosis depends on the effective activation of a cascade of proteases known as caspases. Completion of these pathways leads to the destruction of cellular components, the formation of apoptotic bodies, and their subsequent removal by phagocytes [5]. The Bcl-2 gene family consists of both pro-apoptotic and anti-apoptotic proteins. The Bcl-2 gene encodes a mitochondrial protein that inhibits apoptosis, and its dysfunction has been observed in many cancers [3]. The Bax protein facilitates programmed cell death by activating the intrinsic apoptotic pathway, primarily through its inhibitory interaction with the anti-apoptotic protein Bcl-2 [3, 4]. Bax interacts with membrane proteins, leading to caspase activation, increased mitochondrial membrane permeability, and subsequent apoptosis. In contrast, Bcl-2 exerts an anti-apoptotic effect in response to various apoptotic stimuli [6]. The balance between cell proliferation and apoptosis is disrupted in cancer cells, leading to uncontrolled growth. Therefore, the expression levels of these genes are directly related to cancer development, making them potential therapeutic and diagnostic targets in cancer research [5]. Reactive oxygen species significantly contribute to cancer development, making antioxidants crucial for cancer prevention. Natural antioxidants are preferred, with fungi playing a vital role. For instance, extracts from Ganoderma mycelium and its fruiting bodies exhibit strong antioxidant properties [7]. *Ganoderma lucidum*, a basidiomycete fungus, is renowned for its medicinal benefits, including antidiabetic, antioxidant, antibacterial, antitumor, antimetastatic, cholesterol-lowering, and antihypertensive effects [8]. These effects are attributed to various secondary metabolites of *Ganoderma lucidum*, including polysaccharides, triterpenoids, lectins, peptidoglycans, proteoglycans, and Ganodermin [8, 9]. Polysaccharides and triterpenoids are the two main active components of *Ganoderma lucidum* [9]. The primary challenge in cancer treatment is effectively targeting cancer cells while minimizing harm to healthy cells, underscoring the importance of targeted drug delivery [10, 11]. With advances in nanoscience, researchers have recognized that nanoparticles can be used to diagnose and treat cancers, leading to extensive studies in nano-oncology [12, 13]. Among the nanoparticles of interest are nanocarriers, which include liposomes, niosomes, micelles, dendrimers, polymeric carriers, and chitosan nanoparticles, all employed in targeted drug delivery [12, 14-16]. In modern drug delivery systems, chitosan is widely utilized as a bio-nanocarrier. Recently, researchers have focused on chitosan-based nanocarriers due to their unique biological and physicochemical properties [14, 17-21]. Chitosan demonstrates exceptional properties, including strong adhesion, biodegradability, biocompatibility, and various health benefits, such as antimicrobial, cholesterol-lowering, anticancer, and anti-inflammatory properties. Additionally, it possesses blood-coagulating properties. Chitosan nanoparticles carry a positive charge, which contributes to their strong adhesion and high adsorption capacity, making them especially effective for targeting solid tumors [10, 22-24]. Chitosan offers several advantages over other biopolymers, including high mechanical strength, good biocompatibility, low toxicity, high permeability and solubility in water,

sensitivity to chemical modifications, and cost-effectiveness [10, 24]. Chitosan nanoparticles with a high degree of deacetylation exhibit enhanced permeability into epithelial tissues, small particle size, and a high surface-to-volume ratio, making them excellent nanocarriers for cancer therapy [14, 25, 26]. These nanoparticles can affect cancer cells by interfering with their metabolism and growth, inducing apoptosis, and stimulating the antitumor immune response [10, 27]. Additionally, chitosan nanoparticles possess antioxidant properties that contribute to cancer prevention and reduction [10]. Currently, chitosan-based drug nanocarriers are being developed for multiple administration routes, including oral, nasal, vaginal, and rectal delivery [14, 17]. Chitosan, a component of fungal cell walls such as those of mushrooms, also exhibits intrinsic anticancer effects. When combined with polysaccharides from *Ganoderma lucidum* in nanoparticle form, a synergistic effect may arise, enhancing the suppression of cancer gene expression.

Polysaccharides derived from *Ganoderma lucidum* have been extensively researched for their anticancer properties on various cancer cell lines. Additionally, research has explored chitosan nanoparticles as effective carriers for drugs and anticancer agents. However, studies specifically investigating the combined anticancer effects of these two agents are limited, and most existing studies have focused on different cell lines, making direct comparison difficult. Table 1 lists some related studies. Given the high prevalence of prostate cancer, this study investigated the effects of chitosan nanoparticles containing *Ganoderma lucidum* polysaccharides on apoptosis induction in the PC3 cell line, and the results indicate significant pro-apoptotic activity**.**

2. Materials and Methods

2.1. Preparation of Fungal Bank

Ganoderma lucidum IBRC-M 30306 was obtained from the Iranian Genetic and Biological Resources Center.

2.2. Extraction of *Ganoderma lucidum* Polysaccharide Content

Ganoderma lucidum was powdered under sterile conditions, and 10 g of this powder was treated with 96% ethanol and boiled for nine hours, then dried in an incubator at 62 °C. An aqueous extraction of polysaccharides was subsequently performed. The phenol-sulfuric acid method (Sigma–Aldrich, Germany) was used to analyze the extract's sugar content. Proteins were removed using 1-butanol and chloroform (Merck, Germany). Polysaccharides were precipitated using ethanol and then dried in a freeze-dryer (Christ, Alpha 1-4 LD plus, Germany) [27].

2.3. Preparation of Chitosan Nanoparticles

A solution of chitosan (Sigma–Aldrich, Germany) at 2 mg/mL was prepared using 2% (w/v) acetic acid (Merck, Germany). Separately, a sodium tripolyphosphate solution (Sigma–Aldrich, Germany) was prepared at a concentration of 1 mg/mL. To form the nanoparticles, 2 mL of the sodium tripolyphosphate solution was added dropwise to 5 mL of the chitosan solution, and the mixture was thoroughly stirred, followed by sonication at 80 kHz for 30 minutes (Elmasonic S 80 H, Elma Schmidbauer GmbH, Germany) [38].

2.4. Preparation of Chitosan-Polysaccharide Nanoparticles

The hydrolysis of chitosan involved dissolving 500 mg of chitosan powder in 100 mL of distilled water containing 1% hydrochloric acid, followed by sonication at 80 kHz for 30 minutes. This method was used to hydrolyze the

polysaccharide. Next, 100 mL of the chitosan mixture, containing 500 mg of hydrolyzed chitosan, was added dropwise to the hydrolyzed polysaccharide mixture in 100 mL of phosphate-buffered saline. Then, 10 mg of EDC[1] and NHS[2] (Sigma–Aldrich, Germany) were added and mixed for two hours, followed by sonication [39].

2.5. Investigation of the Properties of the Synthesized Nanoparticles

2.5.1. Fourier-transform infrared spectroscopy (FTIR)

FTIR analysis was conducted to investigate the chemical bonds and functional groups of chitosan-polysaccharide nanoparticles, commercial chitosan samples, and polysaccharide extracts using an infrared spectrometer (BRUKER spectrometer, EQUINOX 55, Germany). Finally, the peaks in the range of 4000-600 cm^{-1} were examined.

2.5.2. Morphology analysis

A thin layer of gold was applied to the nanoparticles to assess their dimensions and morphology. Their dimensions and morphology were evaluated using scanning electron microscopy (TESCAN, Vega 3, Czech Republic) at a magnification of 70,000× [40].

2.6. Cell Culture and Treatment of PC3 Cell Line

The PC3 cell line (catalog number ATCC® CRL-1435) was sourced from the Iranian Genetic Resources Center. It was cultured in DMEM medium enriched with 10% fetal bovine serum, 2 mM glutamine, sodium pyruvate, non-essential amino acids, 100 U/mL penicillin and 100 µg/mL streptomycin (Gibco, Iran). Cultures were maintained at 37 °C in a humidified atmosphere containing 5% CO2. Chitosan-polysaccharide nanoparticles were suspended in serum-free culture medium and subjected to ultrasonication for 5 hours to form a homogeneous suspension. The mixture was then filtered through 0.22 µm syringe filters, and dilutions of 19.53, 39.06, 78.12, 156.25, 312.5, and, 625 µg/mL were prepared in culture medium. Cells were incubated with these nanoparticle dilutions for 24, 48, and, 72 hours. All experiments were conducted in triplicate, and the results are the average of the three replicates.

2.7. Cell Viability Assessment

A 1 mL cell suspension was prepared, and 20 µL of 0.25% Trypan Blue (Sigma–Aldrich, Germany) was added. Then, 10 µL of the mixture was placed onto a Neobar lam (Marienfeld, Germany) for microscopic counting of viable and dead cells. The experiments were conducted in triplicate to ensure accuracy, and the reported results are the averages of these three replicates. The total cell count and viability percentage were calculated using the following formulas [41]:

Number of cells in 1 mL of cell suspension = Volume of suspension × 20000 ×Number of viable cells in W area

$$\%Viability = \frac{\text{Number of viable cells in cell suspension}}{\text{Total number of cells (viable cells } + \text{ dead cells)}} \times 100$$

[1] 1-Ethyl-3-(3-dimethylaminopropyl) carbodiimide (EDC)
[2] N-Hydroxysuccinimide (NHS)

2.8. Cytotoxicity study using MTT assay

Cells were seeded in a 96-well plate at a density of 10^4 cells/well in 100 µL culture medium and incubated for 24 hours. Nanoparticles were administered at concentrations ranging from 19.53 to 625 µg/mL, followed by a 48-hour incubation. The medium was removed, and 20 µL of MTT solution (5 mg/mL; Merck, Germany) was added to each well. Plates were incubated in the dark for 4 hours, after that absorbance was measured at 570 nm using a microplate reader (TECAN Sunrise, USA). Cell viability was calculated relative to untreated controls, and the IC50 concentration was determined via dose-response analysis [26]. All experiments were performed in triplicate, and the results are presented as the mean values of the three independent replicates.

2.9. Analysis of the rate of apoptosis-necrosis of cells

Annexin V and propidium iodide (BioLegend, USA) were used to stain cells for cell death assessment, and subsequently analyzed by flow cytometry using FlowJo software (version 7.6.1)**.**

2.10. Gene expression analysis

The RNA-PLUS kit (CinnaGen, Iran) was used to extract total RNA, and its concentration was determined using a NanoDrop spectrophotometer (Thermo Fisher Scientific, USA). Complementary DNA (cDNA) synthesis was performed with the SinaClon First Strand cDNA Synthesis kit (SinaClon, Iran). Primers for the target genes were designed by Pishgam Company using OligoAnalyzer 3.1 and Primer3Plus (http://www.bioinformatics.nl/cgibin/primer3plus/primer3plus.cgi), and their specificity was confirmed by BLAST (https://blast.ncbi.nlm.nih.gov/Blast.cgi). The primer sequences are provided in Table 2. PCR amplification was carried out in a thermocycler (Thermo Fisher Scientific, USA) under the following cycling conditions: denaturation at 95 °C for 5 seconds, annealing at 60 °C for 1 minute, and extension at 95 °C for 120 seconds.

2.11. Statistical Methods

All experiments were performed in triplicate (n = 3), unless otherwise specified. Data are presented as mean ± standard deviation (SD). Statistical analyses were performed using SPSS software (Version 26). For comparisons among multiple groups, one-way analysis of variance (ANOVA) was used. When significant differences were detected by ANOVA, post hoc pairwise comparisons were conducted to determine specific group differences. For all analyses, a p-value of less than 0.05 was considered statistically significant. Where appropriate, results with $p < 0.01$ and $p < 0.001$ were also reported to indicate stronger levels of significance.

IC50 values for cell viability were calculated using nonlinear regression analysis of dose-response curves from MTT assay data. For gene expression analysis (Bax and Bcl-2), fold changes were quantified using the comparative Ct (ΔΔCt) method, and statistical differences between groups were assessed using ANOVA.

For apoptosis and necrosis rates determined by flow cytometry (Annexin V/PI staining), data were analyzed by ANOVA followed by post hoc tests to compare treated and control groups. Confidence intervals (95% CI) were calculated and reported where relevant to provide precision estimates.

3. Results and discussions

3.1. Sugar content in *Ganoderma Lucidum* extract

The results indicated that 23.77 μg of sugar was present in 1 mL of the *Ganoderma lucidum* extract sample, compared to 3 μg of sugar in 1 mL of the standard glucose solution.

3.2. FTIR data analysis

Chitosan and polysaccharides share similar structural frameworks, resulting in comparable FTIR spectra. The primary distinction between the two is the presence of the amine (NH_2) group in chitosan. As illustrated in Figures 1a and 1b, the absorption peak at 3443 cm^{-1} corresponds to N-H stretching, which overlaps with the O-H stretching peak due to hydrogen bonding. The peak observed at 2900 $cm^{-1}$is attributed to C-H stretching, while the peak at 1550 cm^{-1} is associated with N-H bending and the peak at 1400 cm^{-1} is associated with C–N stretching or O–H bending. Additionally, the peak at 1100 cm^{-1} arises from C-O stretching. The polysaccharide sample lacks functional groups such as carboxyl and aldehyde groups; therefore, no covalent bond formation is expected between the polysaccharide and the amine group of chitosan. This is supported by the FTIR spectra, which show that the characteristic functional groups remain intact. In the spectrum of the chitosan–polysaccharide nanoparticle, the NH_2 peak is prominent but exhibits reduced interaction with O-H groups compared to pure chitosan. This suggests that chitosan envelops the polysaccharide chains, forming hydrogen bonds between their O-H groups, while the NH_2 groups of chitosan are oriented outward. The FTIR spectrum of the resulting nanoparticles is presented in Figure 1c and Table3.

3.3. Morphology of nanoparticles

According to Figure 2a, due to the overlap of the polysaccharide and chitosan structures, the SEM images reveal a homogeneous, nearly cubic morphology, with the grains appearing as square-shaped fibers. In Figure 2b, particles labeled D1, D2, and D3 confirm the presence of nanoparticles within the synthesized composition. WD refers to the working distance, and BL denotes the image mode used for magnification.

3.4. PC3 cell line viability percentage

The cell viability percentages at various concentrations of chitosan-polysaccharide nanoparticles and polysaccharides over 24, 48, and 72 hours, as well as the comparison of cell viability percentages across these time points, are presented in Figures 3a, 3b, 3c, 3d, and 3e, respectively. After 24 hours of exposure to chitosan-polysaccharide nanoparticles, cell viability significantly increased as the nanoparticle concentration decreased. Specifically, at concentrations of 312.5 and 625 μg/mL, a notable decrease in viability was observed, with a significance level of $p < 0.001$. A decrease in viability was also noted at concentrations of 78.12 and 156.25 μg/mL but no significant decrease has been occurred at concentrations of 19.53 and 39.06 μg/mL. Similar decreases in viability were observed in cells treated with polysaccharide, reaching significance levels of $p < 0.01$ and $p < 0.05$, respectively. During the 48-hour incubation, the percentage of cell viability continued to increase as the concentration of chitosan-polysaccharide nanoparticles decreased. A significant decrease in viability was observed at concentrations of 156.25, 312.5, and 625 μg/mL, all at the $p < 0.001$ level. Decreases were also noted at 39.06 and 78.12 μg/mL, although these were less

pronounced. However, no significant decrease in viability was detected at the 19.53 μg/mL concentration. This trend was similarly evident in cells treated with polysaccharide, showing significance at $p < 0.01$ and $p < 0.05$ levels, respectively. After 72 hours of treatment with chitosan-polysaccharide nanoparticles, cell viability increased as concentrations decreased. Significant reductions in viability were observed at concentrations of 625, 312.5, 156.25, and 78.12 μg/mL, all at the $p < 0.001$ level. Additionally, a significant decrease in viability occurred at 39.06 μg/mL ($p < 0.01$), which was also seen in cells treated with polysaccharide alone. Notably, at 19.53 μg/mL, chitosan-polysaccharide nanoparticles caused a significant decrease in viability ($p < 0.05$) compared to the control group, whereas polysaccharide alone did not produce a significant effect at this concentration. In conclusion, extending exposure time to chitosan-polysaccharide nanoparticles from 24 to 72 hours significantly reduced cell viability.

3.5. Flow cytometry results

The flow cytometry analysis results for the control group, the polysaccharide treatment group at sub-IC50 concentration, the polysaccharide treatment group at IC50 concentration, the chitosan-polysaccharide nanoparticle treatment group at sub-IC50 concentration, and the chitosan-polysaccharide nanoparticle treatment group at IC50 concentration are presented in Figures 4a, 4b, 4c, 4d, and 4e, respectively. After a 24-hour treatment, cells exposed to chitosan-polysaccharide nanoparticles and polysaccharide at IC50 and sub-IC50 concentrations exhibited cell cycle arrest across all phases, with a pronounced effect in the sub-G1 and G1 phases. Treatment with chitosan-polysaccharide nanoparticles resulted in a significant increase in cell cycle arrest in the sub-G1 phase ($p < 0.001$), indicating reduced cell viability and enhanced apoptosis induction. In addition, both the chitosan-polysaccharide nanoparticles and the polysaccharide caused a greater arrest in the G1 phase. However, the extent of cell cycle arrest induced by the chitosan-polysaccharide nanoparticles was less than that observed in the control group and also less than that in the polysaccharide treatment group. Moreover, approximately 19% of the cells treated with chitosan-polysaccharide nanoparticles were arrested in the G2 phase, representing a notable increase compared to the polysaccharide treatment, but this difference was not statistically significant compared to the control group. The percentages of cells in each cell cycle phase after 24 hours of treatment with polysaccharide and chitosan-polysaccharide nanoparticles are detailed in Table 4. Additionally, the comparison with the control group is shown in figure 4f.

3.6. Apoptosis/necrosis rate of PC3 cells treated with chitosan-polysaccharide nanoparticles by flow cytometry

The Annexin V/PI flow cytometry histograms for the control group, the polysaccharide treatment group at sub-IC50 concentration, the polysaccharide treatment group at IC50 concentration, the chitosan-polysaccharide nanoparticles treatment group at sub-IC50 concentration, and the chitosan-polysaccharide nanoparticles treatment group at IC50 concentration are presented in figures 5a, 5b, 5c, 5d, and, 5e, respectively. In these plots, the colored dots in quadrant Q1 (upper left) represent necrotic cells, those in Q2 (upper right) indicate late apoptotic cells, the dots in Q3 (lower right) correspond to early apoptotic cells, and the dots in Q4 (lower left) denote live cells. Under treatment with the IC50 concentration of chitosan-polysaccharide nanoparticles, the graph shows the percentage of apoptotic and necrotic PC3 cells, illustrating the extent of cell death induced by this treatment. Approximately 14.8% of PC3 cells treated

with chitosan-polysaccharide nanoparticles underwent early apoptosis, 21.3% underwent late apoptosis, and 2.37% experienced necrosis. In the control group, approximately 0.034% of cells underwent early apoptosis, around 0.068% experienced late apoptosis, and less than 0.034% underwent necrosis. These results demonstrate a significant increase in apoptosis in PC3 cells treated with polysaccharide and chitosan-polysaccharide nanoparticles at both IC50 and sub-IC50 concentrations, with a significance level of $P < 0.001$. This increase is particularly pronounced in secondary apoptosis for cells treated with chitosan-polysaccharide nanoparticles at the IC50 concentration. Similarly, cells treated with polysaccharide at both IC50 and sub-IC50 concentrations showed a significant increase in secondary apoptosis at the same significance level ($P < 0.001$). The percentages of apoptosis and necrosis in cells treated with chitosan-polysaccharide nanoparticles and polysaccharide at IC50 and sub-IC50 concentrations are summarized in Table 5.

3.7. Gene expression

Melting curves for β-actin and amplification curves for Bax and Bcl-2 were generated using the Real-Time PCR StepOne system, as shown in Figures 6a and 6b. The results demonstrated that the expression level of the Bax gene in the treated PC3 cell line sample increased compared to the control sample. Figure 6c presents a comparative graph of Real-Time PCR analysis for the genes Bax, Bcl-2, and β-actin in both treatment and control groups. Bax gene expression was significantly elevated in the group treated with chitosan-polysaccharide nanoparticles compared to the control group, measuring 4.6 units with a p-value ≤ 0.001. Conversely, Bcl-2 gene expression in the chitosan-polysaccharide nanoparticle treatment group showed a significant decrease compared to the control, approximately 0.64 units, with a p-value ≤ 0.05, indicating induction of apoptosis. Besides, increasing the concentration of chitosan-polysaccharide nanoparticles and polysaccharide at the IC50 level significantly has been enhanced Bax expression while reducing Bcl-2 expression. The expression ratio of Bax to Bcl-2 genes in treatments with chitosan-polysaccharide nanoparticles and polysaccharide is summarized in Table 6.

3.8. Discussion

Prostate cancer is recognized as the second most common cancer in men, highlighting the need for early detection and treatment. *Ganoderma lucidum*, an edible mushroom, possesses antidiabetic, antioxidant, and antitumor properties, with its polysaccharides potentially inhibiting tumor growth [8, 39, 42]. Advances in nanotechnology, particularly involving chitosan nanoparticles, have led to improvements in drug delivery due to their biocompatibility [8, 43]. The combination of chitosan with Ganoderma polysaccharides may result in effective suppression of cancer-related gene expression, offering a promising treatment strategy [39].

It is demonstrated that chitosan nanoparticles loaded with *Ganoderma lucidum* polysaccharides (GLP-CSNPs) significantly modulate the expression of apoptosis-related genes in PC3 prostate cancer cells. While these results are aligned with previous studies showing anticancer effects of both *Ganoderma lucidum* and chitosan individually, novel insights into their combined application as a nanocarrier system are provided. A study investigating the direct effects of *Ganoderma lucidum* polysaccharides on cervical cancer cells demonstrated a dose and time-dependent reduction in cell viability [44]. In another study, the biological effects of polysaccharides derived from Lentinula edodes and

Ganoderma lucidum on the MCF-7 breast cancer cell line were examined. The findings demonstrated a dose- and time-dependent increase in p53 gene expression alongside a decrease in HER-3 gene expression [45]. Additionally, the impact of chitosan nanoparticles on the delivery of doxorubicin in ovarian cancer cells was investigated in vitro. Ovarian cancer cells were treated with doxorubicin-loaded chitosan nanoparticles for three days, resulting in enhanced drug uptake and cytotoxicity [6]. In a separate study, chitosan nanoparticles and polysaccharides extracted from *Ganoderma lucidum* increased p53 gene expression while decreasing HER3 gene expression in the MCF-7 cell line, contributing to tumor cell resistance [22]. In the studies referenced in Table 1 and other related research, *Ganoderma lucidum* polysaccharides have been shown to regulate genes involved in the apoptosis pathway, including Bax and Bcl-2. These polysaccharides have been shown to effectively induce apoptosis. Similarly, chitosan nanoparticles are recognized as efficient carriers for delivering drugs and anticancer agents, offering controlled release rates, low toxicity, and antioxidant properties. This study's findings are consistent with earlier investigations and reinforce the existing body of evidence.

The observed 4.6-fold increase in pro-apoptotic Bax expression and 0.64-fold decrease in anti-apoptotic Bcl-2 expression with GLP-CSNPs suggests a synergistic effect that exceeds what has been previously reported with either component alone. For instance, Wang *et al.* (2020) demonstrated only a 2.3-fold increase in Bax expression using free Ganoderma polysaccharides [34], while Zhong *et al.* (2022) reported a 0.75-fold reduction in Bcl-2 using chitosan nanoparticles without bioactive loading [37]. The enhanced effect likely results from improved cellular uptake facilitated by the chitosan nanocarrier and the preserved bioactivity of the polysaccharides within this delivery system. However, limitations that warrant consideration are present in this study. Unlike Xu *et al.* (2017), who tested multiple cancer cell lines, exclusive focus was placed on PC3 cells [33], which limits the generalizability of the findings. Additionally, while changes in gene expression were observed, downstream protein expression or other apoptotic pathways were not investigated as comprehensively as in Jin *et al.* (2020), who examined caspase activation and mitochondrial membrane potential changes [44].

In this study, chitosan was used as a pharmaceutical carrier. The results demonstrated that a polysaccharide was combined with chitosan nanoparticles via an ionic bond copolymerization method. The investigation focused on apoptosis induction by analyzing cellular changes and expression of Bax and Bcl-2. The study also investigated the effects of chitosan-polysaccharide nanoparticles on cell cycle arrest and proliferation in the PC3 cell line. Incubating PC3 cells with these nanoparticles for 24 hours led to a dose-dependent reduction in cell viability, with higher nanoparticle concentrations producing more pronounced effects. Comparable results were observed in cells treated with polysaccharides alone. Treatment with polysaccharides and chitosan-polysaccharide nanoparticles at IC50 and sub-IC50 levels significantly increased cell cycle arrest in the sub-G1 phase ($P < 0.001$), indicating reduced viability and enhanced apoptosis. Furthermore, both treatments upregulated the pro-apoptotic gene Bax while downregulating the anti-apoptotic gene Bcl-2, confirming the induction of apoptosis.

5. Conclusion

As highlighted in the introduction and discussion, and supported by data in Table 1, this study's findings align with previous research. These demonstrate the anticancer properties of polysaccharides extracted from *Ganoderma lucidum*.

Additionally, chitosan nanoparticles, which serve as carriers for these polysaccharides, showed promising results. The study investigated apoptosis induction in PC3 cells using flow cytometry. Treatment with chitosan-polysaccharide nanoparticles and polysaccharides at IC50 and sub-IC50 concentrations significantly induced primary and secondary apoptosis ($p < 0.001$). Notably, the highest level of secondary apoptosis was observed in cells treated with chitosan-polysaccharide nanoparticles compared to other groups. Across all tested methods, including MTT assays, real-time PCR, and flow cytometry, the chitosan-polysaccharide nanoparticles demonstrated greater cytotoxicity. This effect was associated with the upregulated expression of the pro-apoptotic gene Bax and the downregulated expression of the anti-apoptotic gene Bcl-2. These findings suggest that chitosan-polysaccharide nanoparticles hold significant potential as a pharmaceutical formulation for prostate cancer treatment. However, additional invitro studies are needed to further evaluate the expression of other genes and key factors involved in the cell cycle and apoptosis processes, including caspase activity. Moreover, it is recommended to compare the effects of polysaccharide-containing nanoparticles with those of chitosan nanoparticles alone, as well as with positive control agents such as established therapeutic drugs. On the other hand, testing across multiple cancer cell lines and including normal prostate epithelial cells is recommended to enhance the generalizability and relevance of findings. Furthermore, comprehensive toxicological assessments and in vivo studies are essential to confirm both the efficacy and safety of the resulting compounds before progressing to clinical trials.

Acknowledgments

The authors would like to sincerely thank the laboratory staff at Islamic Azad University for their invaluable support and assistance throughout this research.

Authors contributions

ML designed the study, M.B. and M.L. supervised the experiments. M.J. and H.D. performed the experiments. M.L. and M.J. analyzed and interpreted the data. ML supervised the study. H.D. and SSA wrote the first draft of the manuscript. ML and MJ reviewed and implemented the article draft. All the authors read and approved the final manuscript.

Availability of data and materials

The authors affirm that all data supporting the findings of this study are available and accessible upon request.

Conflict of interest

The authors declare that they have no financial or personal conflicts of interest that could have influenced the work presented in this paper.

Reference

[1] Rawla, P. (2019). Epidemiology of prostate cancer. *World journal of oncology, 10*(2), 63. DOI: https://doi.org/10.14740/wjon1191

[2] Al-Hajj, M., Wicha, M. S., Benito-Hernandez, A., Morrison, S. J., & Clarke, M. F. (2003). Prospective identification of tumorigenic breast cancer cells. *Proceedings of the National Academy of Sciences, 100*(7), 3983-3988. DOI: https://doi.org/10.1073/pnas.0530291100

[3] Bagci, E., Vodovotz, Y., Billiar, T., Ermentrout, G., & Bahar, I. (2006). Bistability in apoptosis: roles of bax, bcl-2, and mitochondrial permeability transition pores. *Biophysical journal, 90*(5), 1546-1559. DOI: https://doi.org/10.1529/biophysj.105.068122

[4] Jain, M., Kasetty, S., Khan, S., & Desai, A. (2014). An insight to apoptosis. *J Res Prac Dent*. DOI: https://doi.org/10.5171/2014.372284

[5] Hassan, M., Watari, H., AbuAlmaaty, A., Ohba, Y., & Sakuragi, N. (2014). [Retracted] Apoptosis and molecular targeting therapy in cancer. *BioMed research international, 2014*(1), 150845. DOI: https://doi.org/10.1155/2020/2451249

[6] Javid, A., Ahmadian, S., Saboury, A. A., Kalantar, S. M., & Rezaei-Zarchi, S. (2013). Chitosan-coated superparamagnetic iron oxide nanoparticles for doxorubicin delivery: synthesis and anticancer effect against human ovarian cancer cells. *Chemical biology & drug design, 82*(3), 296-306. DOI: https://doi.org/10.1111/cbdd.12145

[7] Stojković, D. S., Barros, L., Calhelha, R. C., Glamočlija, J., Ćirić, A., Van Griensven, L. J., . . . Ferreira, I. C. (2014). A detailed comparative study between chemical and bioactive properties of Ganoderma lucidum from different origins. *International Journal of Food Sciences and Nutrition, 65*(1), 42-47. DOI: https://doi.org/10.3109/09637486.2013.832173

[8] Wang, H., & Ng, T. (2006). Ganodermin, an antifungal protein from fruiting bodies of the medicinal mushroom Ganoderma lucidum. *Peptides, 27*(1), 27-30. DOI: https://doi.org/10.1016/j.peptides.2005.06.009

[9] Ye, L., Liu, S., Xie, F., Zhao, L., & Wu, X. (2018). Enhanced production of polysaccharides and triterpenoids in Ganoderma lucidum fruit bodies on induction with signal transduction during the fruiting stage. *PLoS One, 13*(4), e0196287. DOI: https://doi.org/10.1371/journal.pone.0196287

[10] Abd Elgadir, M., Uddin, M. S., Ferdosh, S., Adam, A., Chowdhury, A. J. K., & Sarker, M. Z. I. (2015). Impact of chitosan composites and chitosan nanoparticle composites on various drug delivery systems: A review. *Journal of food and drug analysis, 23*(4), 619-629. DOI: https://doi.org/10.1016/j.jfda.2014.10.008

[11] Saeedi, N., & Balali, E. (2024). DFT analyses of diamond-assisted paclitaxel anticancer conjugations and evaluating their features regarding the nano-based drug delivery approach. *International Journal of Nano Dimension, 15*(2). DOI: https://doi.org/10.57647/j.ijnd.2024.1502.13

[12] Azimi, B., Nourpanah, P., Rabiee, M., & Arbab, S. (2014). Producing gelatin nanoparticles as delivery system for bovine serum albumin. *Iranian biomedical journal, 18*(1), 34. DOI: https://doi.org/10.6091/ibj.1242.2013

[13] Habeeb, M., & Vasanthan, M. (2024). Formulation, interaction analysis, and invitro hepatocellular carcinoma studies of Rutin loaded lipid and polymeric nanoparticles. *International Journal of Nano Dimension*. DOI: https://doi.org/10.57647/j.ijnd.2025.1602.09

[14] Sailaja, A. K., Amareshwar, P., & Chakravarty, P. (2010). Chitosan nanoparticles as a drug delivery system. *Res. J. Pharm. Biol. Chem. Sci, 1*(3), 474-484. DOI: https://doi.org/10.1007/978-1-4939-0363-4_11

[15] Wilczewska, A. Z., Niemirowicz, K., Markiewicz, K. H., & Car, H. (2012). Nanoparticles as drug delivery systems. *Pharmacological reports, 64*(5), 1020-1037. DOI: https://doi.org/10.1016/S1734-1140(12)70901-5

[16] Chamundeeswari, M., Jeslin, J., & Verma, M. L. (2019). Nanocarriers for drug delivery applications. *Environmental Chemistry Letters, 17*, 849-865. DOI: https://doi.org/10.1007/s10311-018-00841-1. DOI: https://doi.org/10.1007/s10311-018-00841-1

[17] Matalqah, S. M., Aiedeh, K., Mhaidat, N. M., Alzoubi, K. H., Bustanji, Y., & Hamad, I. (2020). Chitosan nanoparticles as a novel drug delivery system: a review article. *Current drug targets, 21*(15), 1613-1624. DOI: https://doi.org/10.2174/1389450121666200711172536

[18] Moosavi, S. M. R., & Zerafat, M. M. (2021). Fabrication of Gelatin-based natural nanocomposite films using nanoclay and Chitosan for food packaging applications. *International Journal of Nano Dimension, 12*(4). DOI: https://doi.org/10.22034/ijnd.2021.682460

[19] Zargar, V., Asghari, M., & Rajaei, B. (2014). Synthesis and characterization of novel nanocomposite Chitosan membranes for Ethanol dehydration. DOI: https://doi.org/10.7508/ijnd.2014.05.003

[20] Sohrabnezhad, S., Pourahmad, A., Sadjadi, M., & Sadeghi, B. (2008). Nickel cobalt sulfide nanoparticles grown on AlMCM-41 molecular sieve. *Physica E: Low-dimensional Systems and Nanostructures, 40*(3), 684-688. DOI: https://doi.org/10.1016/j.physe.2007.09.081

[21] Zarabadi, S. A., Rahnavard, A., Fahimi, F. G., & Saeb, K. (2025). Utilize Polypropylene-Titanium Dioxide nano-composite, Graphene Oxide-Chitosan-Bentonite nano-absorbent, and straw to remove petroleum hydrocarbons in aquatic environments aggressively. *International Journal of Nano Dimension, 16*(2). DOI: https://doi.org/10.57647/j.ijnd.2025.1602.14

[22] Aruna, U., Rajalakshmi, R., Muzib, Y. I., Vinesha, V., Sushma, M., Vandana, K., & Kumar, N. V. (2013). Role of chitosan nanoparticles in cancer therapy. *Int. J. Innov. Pharm. Res, 4*(3), 318-324. DOI: https://doi.org/10.1007/12_2011_132

[23] Liu, X.-C., Gao, J.-M., Liu, S., Liu, L., Wang, J.-R., Qu, X.-J., . . . Wang, S.-L. (2015). Targeting apoptosis is the major battle field for killing cancers. *World Journal of Translational Medicine, 4*(3), 69-77. DOI: https://doi.org/10.5528/wjtm.v4.i3.69

[24] Inanloo, Z., Yousefi, M., & Baniyaghoob, S. (2025). A novel approach for oral delivery of ZINC using Zinc Sulfate solid lipid nanoparticles. *International Journal of Nano Dimension*. DOI:https://doi.org/10.57647/j.ijnd.2025.1604.28

[25] Kang, L., Gao, Z., Huang, W., Jin, M., & Wang, Q. (2015). Nanocarrier-mediated co-delivery of chemotherapeutic drugs and gene agents for cancer treatment. *Acta Pharmaceutica Sinica B, 5*(3), 169-175. DOI: https://doi.org/10.1016/j.apsb.2015.03.001

[26] Mura, S., Nicolas, J., & Couvreur, P. (2013). Stimuli-responsive nanocarriers for drug delivery. *Nature materials, 12*(11), 991-1003. DOI: https://doi.org/10.1038/NMAT3776

[27] Adhikari, H. S., & Yadav, P. N. (2018). Anticancer activity of chitosan, chitosan derivatives, and their mechanism of action. *International Journal of Biomaterials, 2018*(1), 2952085. DOI: https://doi.org/10.1155/2018/2952085

[28] Li, N., Hu, Y.-L., He, C.-X., Hu, C.-J., Zhou, J., Tang, G.-P., & Gao, J.-Q. (2010). Preparation, characterisation and anti-tumour activity of Ganoderma lucidum polysaccharide nanoparticles. *Journal of pharmacy and pharmacology, 62*(1), 139-144. DOI: https://doi.org/10.1211/jpp.62.01.0016

[29] Rejinold, N. S., Muthunarayanan, M., Muthuchelian, K., Chennazhi, K., Nair, S. V., & Jayakumar, R. (2011). Saponin-loaded chitosan nanoparticles and their cytotoxicity to cancer cell lines in vitro. *Carbohydrate Polymers, 84*(1), 407-416. DOI: https://doi.org/10.1016/j.carbpol.2010.11.056

[30] Liang, Z., Yi, Y., Guo, Y., Wang, R., Hu, Q., & Xiong, X. (2014). Chemical characterization and antitumor activities of polysaccharide extracted from Ganoderma lucidum. *International journal of molecular sciences, 15*(5), 9103-9116. DOI: https://doi.org/10.3390/ijms15059103

[31] Yang, G., Yang, L., Zhuang, Y., Qian, X., & Shen, Y. (2016). Ganoderma lucidum polysaccharide exerts anti-tumor activity via MAPK pathways in HL-60 acute leukemia cells. *Journal of Receptors and Signal Transduction, 36*(1), 6-13. DOI: https://doi.org/10.3109/10799893.2014.970275

[32] Mirzaie, Z. H., Irani, S., Mirfakhraie, R., Atyabi, S. M., Dinarvand, M., Dinarvand, R., . . . Atyabi, F. (2016). Docetaxel–chitosan nanoparticles for breast cancer treatment: cell viability and gene expression study. *Chemical biology & drug design, 88*(6), 850-858. DOI: https://doi.org/10.1111/cbdd.12814

[33] Xu, F., Li, X., Xiao, X., Liu, L.-f., Zhang, L., Lin, P.-p., . . . Li, Q.-s. (2017). Effects of Ganoderma lucidum polysaccharides against doxorubicin-induced cardiotoxicity. *Biomedicine & Pharmacotherapy, 95*, 504-512. DOI: https://doi.org/10.1016/j.biopha.2017.08.118

[34] Wang, X., Wang, B., Zhou, L., Wang, X., Veeraraghavan, V. P., Mohan, S. K., & Xin, F. (2020). Ganoderma lucidum put forth anti-tumor activity against PC-3 prostate cancer cells via inhibition of Jak-1/STAT-3 activity. *Saudi journal of biological sciences, 27*(10), 2632-2637. DOI: https://doi.org/10.1016/j.sjbs.2020.05.044

[35] Saravanakumar, K., Mariadoss, A. V. A., Sathiyaseelan, A., Venkatachalam, K., Hu, X., & Wang, M.-H. (2021). pH-sensitive release of fungal metabolites from chitosan nanoparticles for effective cytotoxicity in prostate cancer (PC3) cells. *Process Biochemistry, 102*, 165-172. DOI: https://doi.org/10.1016/j.procbio.2020.12.005

[36] Abdel-Hakeem, M. A., Abdel-Haseb, O. M., Abdel-Ghany, S. E., Cevik, E., & Sabit, H. (2020). Doxorubicin loaded on chitosan-protamine nanoparticles triggers apoptosis via downregulating Bcl-2 in breast cancer cells. *Journal of Drug Delivery Science and Technology, 55*, 101423. DOI: https://doi.org/10.1016/j.jddst.2019.101423

[37] Zhong, M., Huang, J., Mao, P., He, C., Yuan, D., Chen, C., . . . Zhang, J. (2022). Ganoderma lucidum polysaccharide inhibits the proliferation of leukemic cells through apoptosis. *Acta Biochimica Polonica, 69*(3), 639-645. DOI: https://doi.org/10.18388/abp.2020_6070

[38] Ataollahi, H., & Sadri, M. (2021). Comparison of extraction, optimization and purification of Lentinan in Fruiting body and Mycelium of Lentinula edodes. *Modares Journal of Biotechnology, 12*(4), 110-127. URL: http://biot.modares.ac.ir/article-22-49177-fa.html

[39] Larypoor, M., Bikhof Torbati, M., Alipashazadeh, A., & Akbarzadeh, Y. (2024). The synergistic effects of chitosan and Ganoderma Lucidum nanoparticles on p53 and HER3 gene expression. *International Journal of Molecular and Clinical Microbiology, 14*(2), 2061-2071. DOI: https://doi.org/10.22034/ijmcm.2024.710128

[40] Sadeghi, B., & Vahdati, R. (2012). Comparison and SEM-characterization of novel solvents of DNA/carbon nanotube. *Applied surface science, 258*(7), 3086-3088. DOI: https://doi.org/10.1016/j.apsusc.2011.11.042

[41] Kamiloglu, S., Sari, G., Ozdal, T., & Capanoglu, E. (2020). Guidelines for cell viability assays. *Food frontiers, 1*(3), 332-349. DOI: https://doi.org/10.1002/fft2.44

[42] Kladar, N. V., Gavarić, N. S., & Božin, B. N. (2016). Ganoderma: insights into anticancer effects. *European Journal of Cancer Prevention, 25*(5), 462-471. DOI: https://doi.org/10.1097/CEJ.0000000000000204

[43] R Kamath, P., & Sunil, D. (2017). Nano-chitosan particles in anticancer drug delivery: an up-to-date review. *Mini reviews in medicinal chemistry, 17*(15), 1457-1487. DOI: https://doi.org/10.2174/1389557517666170228105731

[44] Jin, H., Song, C., Zhao, Z., & Zhou, G. (2020). Ganoderma lucidum polysaccharide, an extract from ganoderma lucidum, exerts suppressive effect on cervical cancer cell malignancy through mitigating epithelial-mesenchymal and JAK/STAT5 signaling pathway. *Pharmacology, 105*(7-8), 461-470. DOI: https://doi.org/10.1159/000505461

[45] Larypoor, M. (2022). Investigation of HER-3 gene expression under the influence of carbohydrate biopolymers extract of shiitake and reishi in MCF-7 cell line. *Molecular biology reports, 49*(7), 6563-6572. DOI: https://doi.org/10.1007/s11033-022-07496-w

Figure Captions

Figure 1. a. FTIR spectrum of chitosan. b. FTIR spectrum of polysaccharide. c. FTIR spectrum of chitosan nanoparticles – polysaccharide.

Figure 2. Electron microscope image of synthesized nanoparticles. a. Image with magnification kx50. b. Image with magnification kx200.

Figure 3. Percentage of viability of the PC3 cell line. a. Percentage of viability at different concentrations of chitosan-polysaccharide nanoparticles and polysaccharide for 24 hours. b. for 48 hours. c. for 72 hours. d. Percentage of viability at different concentrations of chitosan-polysaccharide nanoparticles for 24, 48 and 72 hours. e. Percentage of viability at different concentrations of polysaccharide for 24, 48 and 72 hours (*p-values ranging from < 0.05 to < 0.001*).

Figure 4. Results from flow cytometry. a. Control group. b. Treated with polysaccharide sub-IC50. c. Treated with polysaccharide IC50. d. Treated with chitosan-polysaccharide nanoparticles sub-IC50. e. Treated with chitosan-polysaccharide nanoparticles IC50. f. Comparison of results (*$p < 0.001$*).

Figure 5. Annexin/PI histogram in flow cytometry test. a. Control group. b. Treated with polysaccharide sub-IC50. c. Treated with polysaccharide IC50. d. Treated with chitosan-polysaccharide nanoparticles sub-IC50. e. Treated with chitosan-polysaccharide nanoparticles IC50 (*$p < 0.001$*).

Figure 6. Results of gene expression analysis. a. Melting curve of the internal control β-actin gene. b. Amplification curve of the Bax gene and the Bcl-2 gene. c. Comparative graph of Real-Time PCR for the expression of Bax (*p-value ≤ 0.001*) and Bcl-2 genes (*$p \leq 0.05$*).

Table Captions

Table 1. Overview of related studies conducted**.**

Table 2. Primers used in the Real-Time PCR reaction**.**

Table 3. Results from FTIR spectra**.**

Table 4. Percentage of cell population in each phase of the cell cycle in the control and treatment groups after 24 hours of treatment with chitosan-polysaccharide nanoparticles and polysaccharide**.**

Table 5. Percentage of apoptosis and necrosis in cells treated with chitosan nanoparticles, Polysaccharide and polysaccharide at IC50 and sub-IC50 concentrations.

Table 6. Ratio of expression of Bax and Bcl-2 genes in treatment groups with chitosan-polysaccharide nanoparticles and polysaccharide.

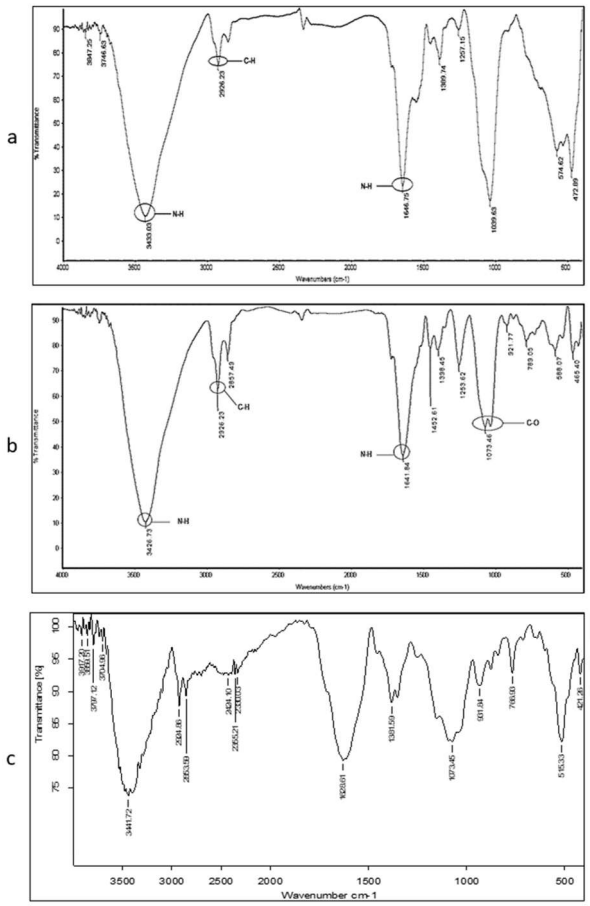

Figure 1. a. FTIR spectrum of chitosan. b. FTIR spectrum of polysaccharide. c. FTIR spectrum of chitosan nanoparticles – polysaccharide.

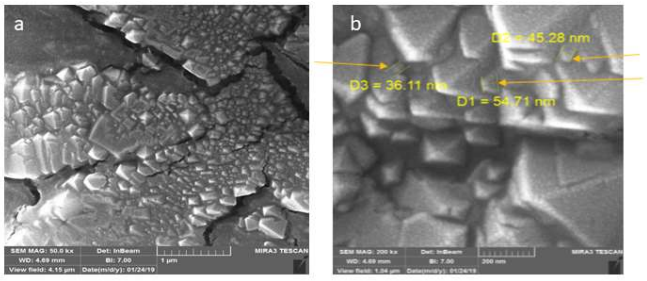

Figure 2. Electron microscope image of synthesized nanoparticles. a. Image with magnification kx50. b. Image with magnification kx200.

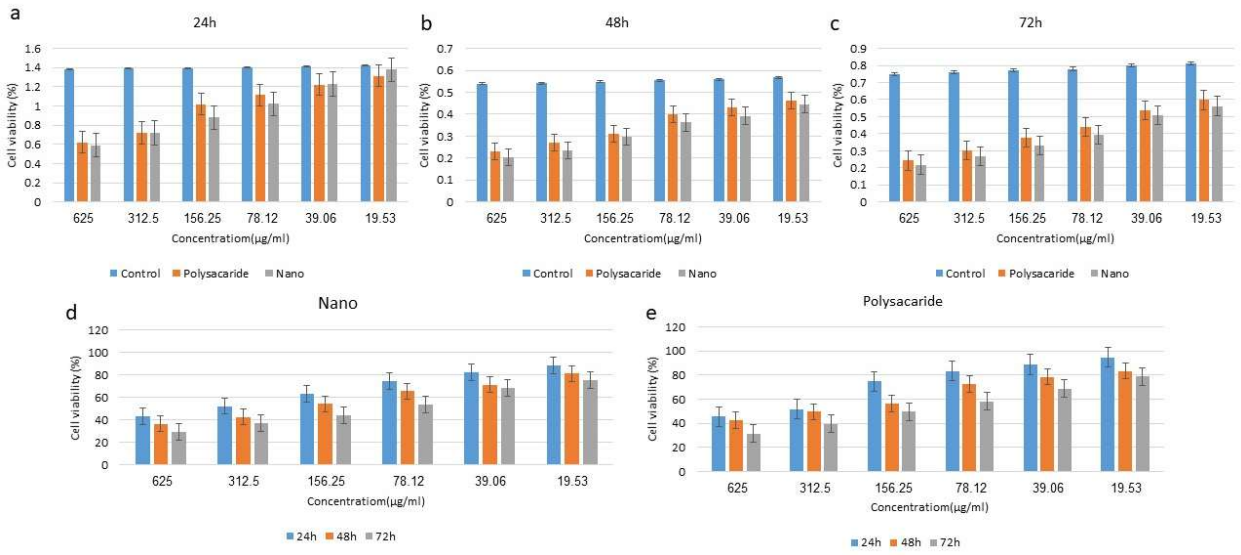

Figure 3. Percentage of viability of the PC3 cell line. a. Percentage of viability at different concentrations of chitosan-polysaccharide nanoparticles and polysaccharide for 24 hours. b. for 48 hours. c. for 72 hours. d. Percentage of viability at different concentrations of chitosan-polysaccharide nanoparticles for 24, 48 and 72 hours. e. Percentage of viability at different concentrations of polysaccharide for 24, 48, and 72 hours (*p-values ranging from < 0.05 to < 0.001*).

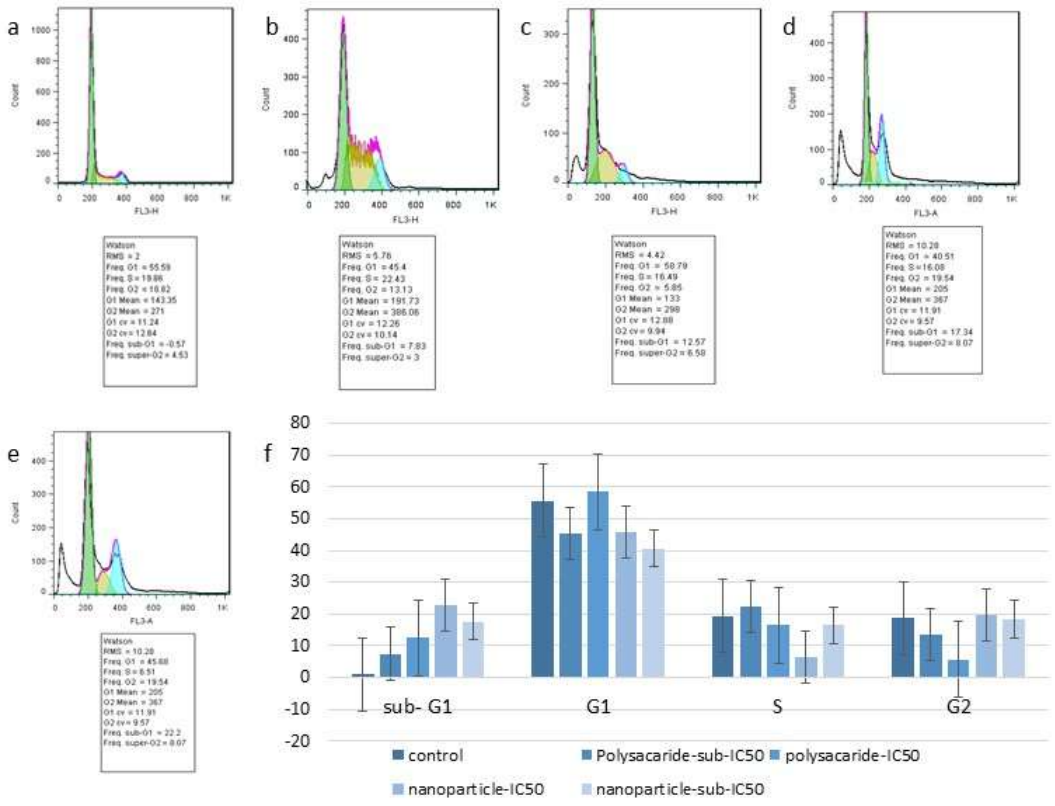

Figure 4. Results from flow cytometry. a. Control group. b. Treated with polysaccharide sub-IC50. c. Treated with polysaccharide IC50. d. Treated with chitosan-polysaccharide nanoparticles sub-IC50. e. Treated with chitosan-polysaccharide nanoparticles IC50. f. Comparison of results (*p < 0.001*).

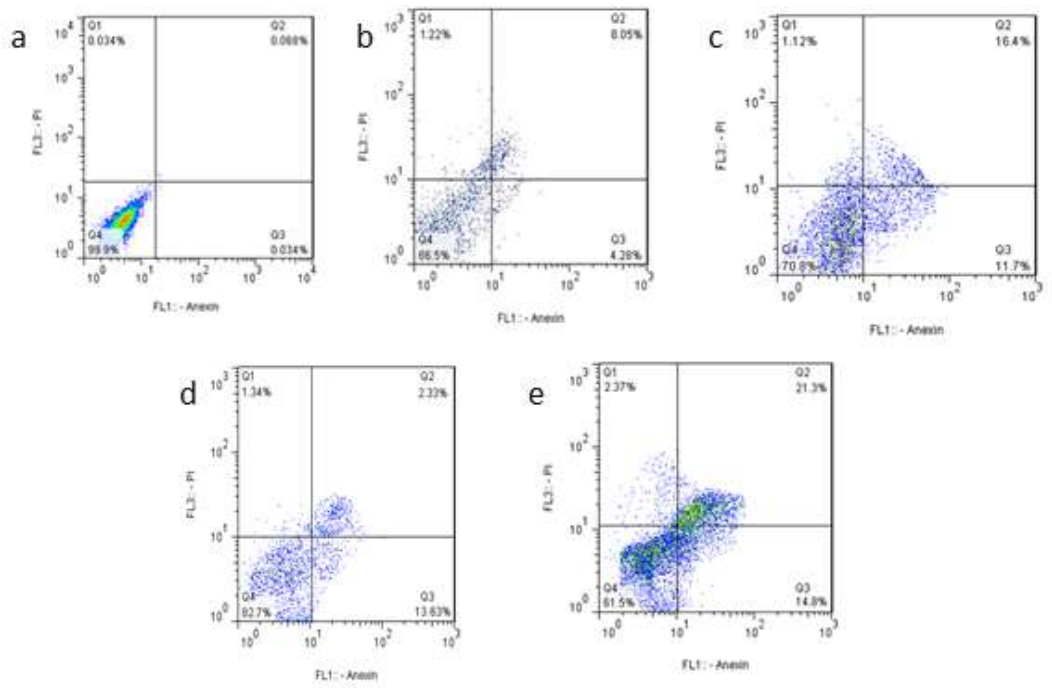

Figure 5. Annexin/PI histogram in flow cytometry test. a. Control group. b. Treated with polysaccharide sub-IC50. c. Treated with polysaccharide IC50. d. Treated with chitosan-polysaccharide nanoparticles sub-IC50. e. Treated with chitosan-polysaccharide nanoparticles IC50 (*p < 0.001*).

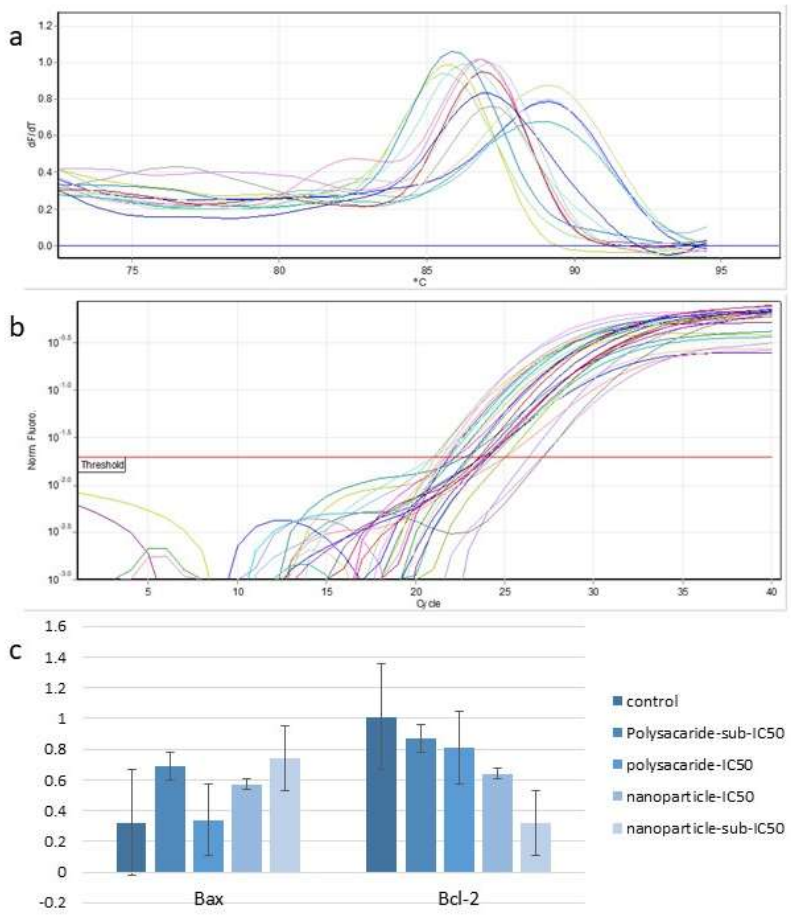

Figure 6. Results of gene expression analysis. a. Melting curve of the internal control β-actin gene. b. Amplification curve of the Bax gene and the Bcl-2 gene. c. Comparative graph of Real-Time PCR for the expression of Bax (*p-value ≤ 0.001*) and Bcl-2 genes (*p ≤ 0.05*).

Table 1. Overview of related studies conducted.

Authors/Year	Summary of the study	Results	Reference
Ni Li, *et al.* / 2010	Preparation of novel *Ganoderma lucidum* polysaccharide nanoparticles and evaluation of physicochemical properties and antitumor activity in in vitro cytotoxicity studies using HepG2, HeLa, and A549 cancer cell lines and growth-enhancing effects on mouse spleen cells	*G. lucidum* polysaccharide-loaded nanoparticles at a concentration of 6 µg/mL and a chitosan/sodium tripolyphosphate (mass) ratio of 5.5 had greater cytotoxic (cell toxicity) effects on tumor cells and growth-enhancing effects on mouse spleen cells than empty nanoparticles.	[28]
N. Sanoj Rejinold,*et al.* / 2011	Development of a Nanoformulation for Anticancer Saponin with Chitosan for Improved and Sustained Release	Cytotoxicity of nanoparticles was investigated on L929, NIH-3T3, KB, and PC3, which showed that the particles were non-toxic in the concentration range of 0.1 to 1.0 mg/mL, while nanosaponin showed specific toxicity on PC3 and KB cell lines.	[29]
Zengenni Liang, *et al.*/2014	Identifying what *Ganoderma lucidum* polysaccharide is doing to inhibit and induce apoptosis in HCT-116 cells.	Bax/Bcl-2, caspase-3, and PARP were expressed more in response to *Ganoderma lucidum* polysaccharide.	[30]
Guohua Yang *et al.*/ 2016	In vitro and in vivo research has been conducted on HL-60 acute myeloid leukemia cells with polysaccharides obtained from *Ganoderma lucidum*.	*Ganoderma lucidum* polysaccharide (GLP) blocks the extracellular signal-regulated kinase/MAPK signaling pathway, simultaneously activating the p38 and JNK MAPK pathways, and thus regulating their downstream genes and proteins, including Bcl-2, p53, Bax, and cyclin D1.	[31]
Zahra H. Mirzaie, *et al.* /2016	Investigation of Docetaxel-containing Nanoparticles and Their Effects on BCL-2 and BAX Gene Expression in Breast Cancer	BAX and BCL-2 gene expression was decreased in nanoparticle-treated cells compared to healthy cells, while the BAX/BCL-2 ratio was significantly increased compared to cells treated with free drug after 72 hours.	[32]
Fan Xu, *et al.* /2017	Studying the effect of *Ganoderma lucidum* polysaccharides (GLPS) on the cardiovascular consequences of DOX	Rat H9c2 cardiomyocytes were treated in the presence of GLPS, which resulted in decreased expression of P53 and p-P65 and increased levels of	[33]

		MDM2 and HO-1, which resulted in reduced apoptosis, oxidative stress, and inflammation induced by DOX. In general, GLPS treatment alleviates H9c2 cell death caused by DOX, and GLPS pretreatment has a significant impact on reducing all the negative effects of DOX.	
Xiaoming Wang, *et al.* /2020	Examining whether *Ganoderma lucidum* has anticancer properties for prostate cancer cells (PC-3) by modifying the JAK-1/STAT-3 signaling pathway	BCL-2 and cyclin-D1 expression are upregulated in PC-3 cells when *Ganoderma lucidum* inhibits STAT-3 transduction, which causes cytotoxicity, increased ROS, and apoptosis.	[34]
Kandasamy Saravanakumar, *et al.* /2020	Trichoderma atroviride metabolite (TM2) has been reported as an anti-prostate cancer agent. This study aimed to load different concentrations of TM2 (1.25-20 mg/mL) into chitosan nanoparticles (TM2-CNPs) to improve its cytotoxicity in PC3 cells.	The IC50 dose of TM2-CNPs treatment induced 60.48% cell death in PC3 cells through caspase-3 activation and inhibition of BCL-2 expression.	[35]
Mohamed A., *et al.* / 2020	Investigation of the ability of the composite to induce apoptosis of doxorubicin (DOX) loaded on chitosan-protamine nanoparticles (CPNPs) in MDA-MB-231 breast cancer cells	The results showed a significant decrease in cell viability/number after treatment, growth arrest of breast cancer cells in G2/M (47.18%), and a decrease in Bcl-2 expression in CPNPs-DOX treatment.	[36]
Mingxing Zhong, *et al.*/ 2022	The investigation will examine the effects of *Ganoderma lucidum* polysaccharides on T-lymphocyte leukemic cells.	Treatment with *G. lucidum* polysaccharide fraction 5 (GLP5) at concentrations of 25 and 50 mg/L resulted in significant increases and decreases in the expression levels of BAX and Bcl2 in Jurkat cells, respectively.	[37]

Table 2. Primers used in the Real-Time PCR reaction.

Gene	Primer Type	Sequence	TM (°C)	Length
β-actin	Forward	5'- TCCTCCTGAGCGCAAGTAC-3'	59.11	19
	Revers	5'- CCTGCTTGCTGATCCACATCT-3'	60.41	21
Bax	Forward	5'- GAGCTGCAGAGGATGATTGC-3′	59.05	20
	Revers	5'- AAGTTGCCGTCAGAAAACATG-3'	57.65	21
Bcl-2	Forward	5'- ATTGGGAAGTTTCAAATCAGC-3′	54.98	21
	Revers	5'- CAGTCTACTTCCTCTGTGATGTTG-3'	58.83	24

Table 3. Results from FTIR spectra**.**

Sample	Peak Position (cm^{-1})	Assignment	Intensity/Shape	Interpretation
chitosan	3443.03	N-H/O-H stretching	Broad	Hydrogen bonding, overlap with O-H
	2926.23	C-H stretching	Moderate	Ring substituent
	1646.75	N-H bending	Moderate	Amide/amine group
	1039.63	C-O stretching	Moderate	Polysaccharide backbone
	1389.74	C–N stretching or O–H bending	Moderate	Amine or hydroxyl group interaction
Polysaccharide	3426.73	O-H stretching	Broad	Hydrogen bonding
	2926.23	C-H stretching	Moderate	Ring substituent
	1641.84	(Absent or weak)	—	Lacks NH2 group
	1073.46	C-O stretching	Moderate	Polysaccharide backbone
	1398.45	C–N stretching or O–H bending	Moderate	Amine or hydroxyl group interaction
Chitosan nanoparticles – polysaccharide	3441.72	N-H/O-H stretching	Broader, less intense	Reduced H-bonding with NH2, more exposed NH2
	2853.59	C-H stretching	Moderate	Ring substituent
	1628.61	N-H bending (doublet)	Split/doublet	NH2 is less involved in H-bonding, more exposed
	1073.45	C-O stretching	Moderate	Polysaccharide backbone

	1381.59	C–N stretching or O–H bending	Moderate	Amine or hydroxyl group interaction

Table 4. Percentage of cell population in each phase of the cell cycle in the control and treatment groups after 24 hours of treatment with chitosan-polysaccharide nanoparticles and polysaccharide.

	control	Polysacaride-sub-IC50	Polysacaride-IC50	Nanoparticle-IC50	Nanoparticle-sub-IC50
sub- G1	1.11	7.53	12.5	22.85	17.66
G1	55.71	45.43	58.60	45.96	40.65
S	19.49	22.45	16.49	6.59	16.48
G2	18.71	13.56	5.76	19.67	18.43

Table 5. Percentage of apoptosis and necrosis in cells treated with chitosan nanoparticles, Polysaccharide, and polysaccharide at IC50 and sub-IC50 concentrations.

	control	Polysacaride-sub-IC50	Polysacaride-IC50	Nanoparticle-IC50	Nanoparticle-sub-IC50
Early	0.83	4.86	11.67	15.26	14.20
Late	0.29	8.88	17.56	21.55	2.81
necrosis	0.13	1.31	1.93	3.28	2.23
Early+ Late	1.12	13.74	29.23	36.81	17.01

Table 6. Ratio of expression of Bax and Bcl-2 genes in treatment groups with chitosan-polysaccharide nanoparticles and polysaccharide.

	control	Polysacaride-sub-IC50	polysacaride-IC50	nanoparticle-IC50	nanoparticle-sub-IC50
Bax	0.32±1.03	0.69±1.75	0.34±2.56	0.57±4.6	0.74±2.82
Bcl-2	1.01±0.27	0.87±0.19	0.81±0.22	0.64±0.25	0.32±0.82